Journal of GeoEngineering, Vol. 17, No. 3, pp. 143-151, September 2022
http://dx.doi.org/10.6310/jog.202209_17(3).3

OPTIMIZED DESIGN OF LINING STRUCTURE FOR HIGH-FILLED CUT-AND-COVER TUNNELS IN THE PLATEAU REGION OF NORTHWEST CHINA

Li Ma [1], Shupei Wang [2], I-Hsuan Ho [3*], Qicai Wang [4], Sheng Li [4], Zhugang You [5], and Changdan Wang [6]

ABSTRACT

High-filled cut-and-cover tunnels (HFCCTs) provide an ideal solution for reclaiming usable land in northwestern China due to the unique landforms of the Loess Plateau. To improve the safety and minimize the cost of such tunnels, most current methods focus on load reduction or a soil arching effect to reduce the earth pressure on cut-and-cover tunnels (CCTs). Although optimizing the design of HFCCTs is an important topic, very few studies have focused on modifying the cross-section of CCTs to improve their design. The modifications of cross-sectional design were proposed, and the vault optimization factor, F, was introduced. The optimal cross-sectional design of a CCT was determined using the finite element method. The experimental results verify that changes to the cross-section of a CCT's lining structure can both reduce the required thickness of the CCT's structure and increase the allowable backfill height above the CCT. The optimization is accomplished by modifying the cross-sectional design of a CCT to minimize the bending moment and allow the CCT to carry a more axially compressive load.

Key words: High-filled cut-and-cover tunnel (HFCCT), optimal cross-sectional design, soil-CCT interaction, vault optimization factor, thickness.

1. INTRODUCTION

High-filled cut-and-cover tunnels (HFCCTs) serve to reclamation of valuable and usable land for high-speed railway construction projects in northwestern China. The amount of backfill required for a cut-and-cover tunnels (CCT) is massive in the Northwest Loess Plateau, which is a mountainous region with deep valleys. Such large amounts of backfill material increase the earth pressure on the HFCCTs significantly, which in turn increases both the vertical and horizontal stress around such HFCCTs. Therefore, compared to conventional CCTs, the required thickness of the lining structure of HFCCTs must be greater. However, when a thicker lining is used, the concrete can crack due to shrinkage after hardening, which also significantly affects the durability of the tunnel structure. In short, both internal forces and the thickness of the lining affect the integrity of CCTs.

Manuscript received September 13, 2021; revised May 30, 2022; accepted June 28, 2022.
[1] Senior Lecturer, College of Civil Engineering, Lanzhou Jiaotong University, China.
[2] M.S student, College of Civil Engineering, Lanzhou Jiaotong University, Lanzhou 730070, Gansu, China.
[3*] Associate Professor (corresponding author), Harold Hamm School of Geology and Geological Engineering, University of North Dakota, 81 Cornell St. Stop. 8358, Grand Forks 58202, North Dakota, USA (e-mail: ihsuan.ho@und.edu).
[4] Professor, College of Civil Engineering, Lanzhou Jiaotong University, Lanzhou 730070, Gansu, China.
[5] M.S student, College of Civil Engineering, Lanzhou Jiaotong University, Lanzhou 730070, Gansu, China.
[6] Associate Professor, Department of Urban Rail Transit and Railway Engineering, College of Transportation Engineering, Tongji University, Shanghai 201804, China.

Early studies analyzed load reduction mechanisms for backfill soils over pipes and culverts (Marston 1922) and focused on different load reduction measures to reduce the earth pressure; such measures include leaves (Spangler 1958), baled straw (Larsen and Hendrickson 1962; Taylor 1973), sawdust or woodchips (McAffee and Valsangkar 2004), and expanded polystyrene (Sladen and Oswell 1988; Vaslestad 1990; Vaslestad and Johansen 1993; Roh *et al.* 2000; Gu *et al.* 2005; Zhang *et al.* 2006; Sun *et al.* 2009; McGuigan and Valsangkar 2010; Meguid *et al.* 2017). Later, these load reduction measures and mechanisms used relatively low-compacted soil (Liedberg 1997) and geogrid (Zaeske 2001; Palmeira and Andrade 2010; Zheng *et al.* 2011; Mehrjardi *et al.* 2013; Van Eekelen *et al.* 2013; Ahmed *et al.* 2015; El Naggar *et al.* 2015; Villard *et al.* 2016) for deeply buried culverts and were applied also to reduce loads on HFCCTs (Li *et al.* 2016a, 2016b, 2019a, 2019b, 2020a). However, very limited research has been conducted to investigate different structural geometries, and very few studies have been focused on structural optimization to reduce the required thickness of buried structures. In addition, some of the aforementioned load reduction methods have been discontinued by some jurisdictions throughout North America due to pipe failure, uncertainties surrounding the design method, or issues related to constructability (McAffee and Valsangkar 2008). Therefore, alternative methods are needed to reduce earth pressure to ensure the safety of such tunnel structures.

The cross-sectional design of culvert has been found to have a significant effect on improving the internal forces that are subjected to the distribution of earth pressure (Vladimir *et al.* 2013). For HFCCTs, different cross-sectional designs have been found to have different effects on the earth pressure distribution and soil arching after load reduction (Li *et al.* 2020b). The objectives of this study are to determine a feasible and optimal cross-section design that considers the interaction of the soil and buried structure, modify the geometry of a HFCCT's lining structure, reduce the required thickness of the lining structure based on the mechanical characteristics of the optimized structure, improve the safety of the lining structure, and increase the allowable backfill height. We employed the finite element code ANSYS to investigate the optimization of the cross-section of a CCT lining structure. The optimized cross-sectional design was determined based on the distributed internal forces and the required thickness of the lining structure. We also performed laboratory tests of the optimized cross-section design to validate the results of the numerical analyses. The experimental and numerical analysis results was compared, as discussed herein.

2. NUMERICAL ANALYSIS

To investigate the complex interactions between the backfill soil and the structure of a CCT, and thus to determine an optimal design for HFCCTs, we employed the finite element method for numerical analysis. For this analysis, the lining thickness of this study is obtained by iterative calculation. In the calculation process, the change of the lining thickness of the CCT affects the deformation law of the structure, and then affects the structural internal force of the CCT. The lining thickness of the CCT is obtained again until the lining thickness is consistent. Therefore, the internal force and lining thickness of the CCT are obtained through repeated iterative calculation. We conducted similar analyses for different cross-sectional designs of CCTs.

2.1 Finite Element Analysis

We employed ANSYS, which is based on the finite element method, for the numerical analysis in this study. The two-dimensional finite element analysis was used to conduct the internal force of HFCCT lining structure studies. Figures 1(a) to 1(d) shows the numerical model in natural state, CCT construction state,

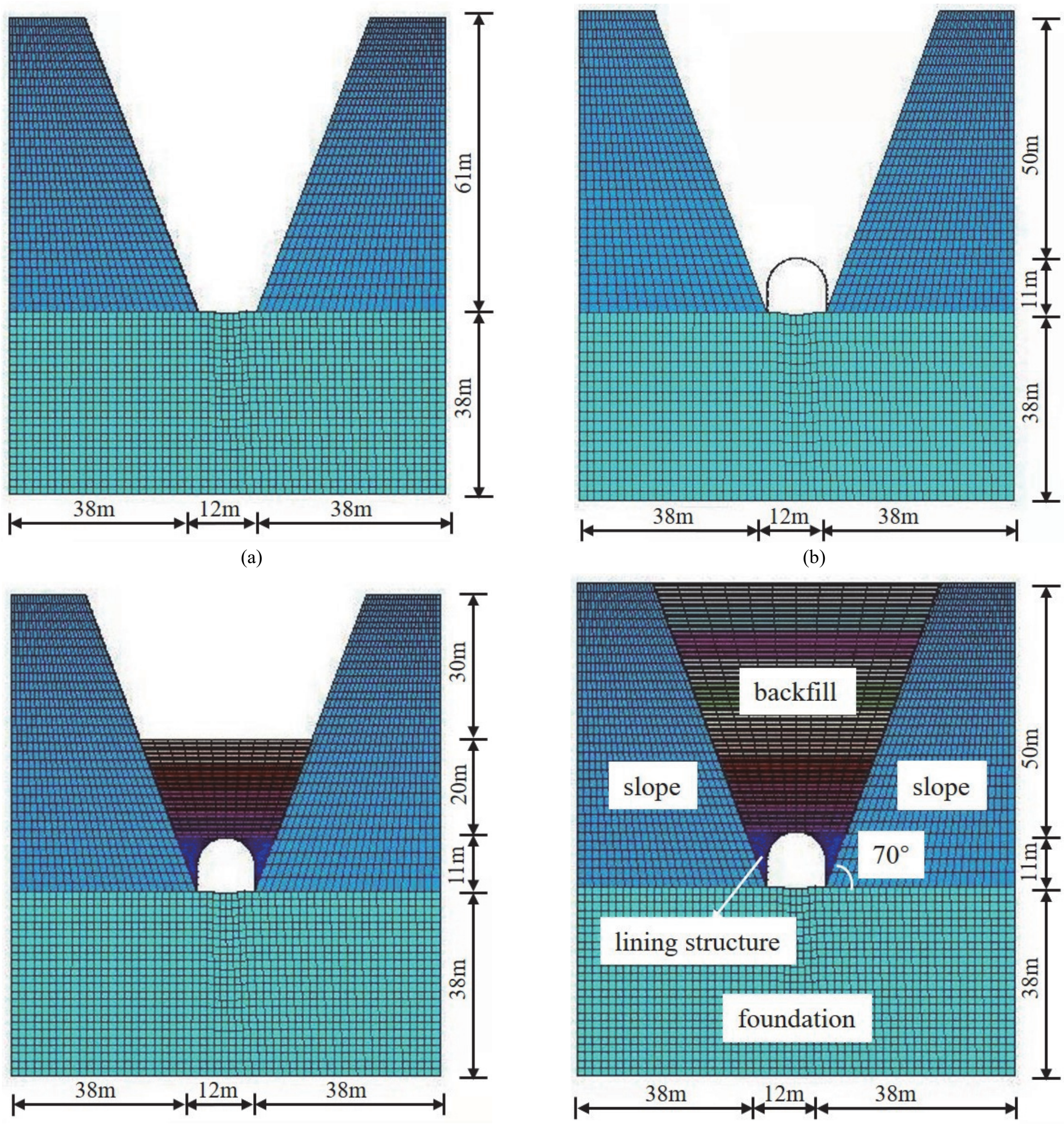

Fig. 1 Finite element model and meshes: (a) natural state, (b) CCT construction state, (c) partial backfill state, and (d) backfill completion state

partial backfill state and backfill completion state, where the default slope angle of the trench is 70°. The element used to model the backfill, CCT, foundation, and slope is plane-strain. For the boundary conditions, the two vertical boundaries are only restrained horizontally, with a fixed bottom. We modeled the CCT and slope using linearly elastic materials and modeled the backfill and foundation soil beneath the CCT using the Mohr-Coulomb elastoplastic failure criterion, for the backfill soil, the relative compaction (R) value of each layer is R = 85%. This paper studies the CCT are usually constructed in natural states. For these natural loess slopes in natural valleys, the lateral supports are not needed since they are not the cases with excavations and then filled. The specific parameters of loess used in the study are as follows: the optimal moisture content ω is 15.25%，the cohesion c is 25 kPa, the maximum dry density ρ_d is 1.925 g/cm^3 , the internal friction angle ϕ is 24°, and the specific gravity of soil particles G_s is 2.69. In the calculation, the lining structure of the CCT is C30 concrete and six ∅22 steel reinforcement with spacing 150 mm.

Table 1 provides a summary of all the required parameters used in the numerical analysis. In the finite element analysis, the interface elements between the soil and structure were simulated using the contact element CONTA172 (backfill) and the target element TARGE169 (structure), which are defaults in ANSYS (McGuigan and Valsangkar 2011a, 2011b; El Naggar *et al.* 2015).

Table 1 Material parameters for finite element analysis

Material	Young's modulus (MPa)	Poisson's ratio	Cohesion (kPa)	Friction angle (°)	Unit weight (kN/m^3)
Backfill	5.4	0.3	31.11	28.24	17.7
Cut-and-cover tunnel	3×10^4	0.167	–	–	24
Foundation	50	0.25	78	32	20
Slope	4×10^3	0.2	–	–	22

2.2 Analysis of Conventional Cut-and-Cover Tunnel

Figure 2 shows a conventionally designed cross-section of a CCT, where the internal forces and thicknesses in the radial direction of the CCT's lining structure are at four locations labeled vault, spandrel, hance, and side wall. We conducted mechanical analysis based on this geometry.

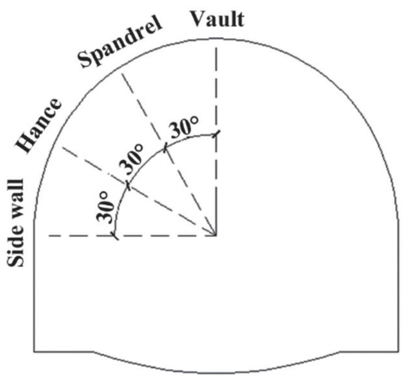

Fig. 2 Cross-sectional design of a conventional CCT's lining structure

2.2.1 Internal Forces of Lining Structure

Figures 3(a) and 3(b) show the relationship between the backfill height and the bending moment and axial force, respectively. These results show that the absolute values of the bending moment increase linearly at the vault (83.02 kN·m/m), side wall (75.65 kN·m/m), spandrel (55.82 kN·m/m), and hance (43.29 kN·m/m) when the backfill height is increased. The axial force rate of increase is in the order of side wall (74.68 kN/m), hance (66.39 kN/m), spandrel (38.98 kN/m), and vault (25.77 kN/m). The analysis results show that the increasing rate of the bending moment is greater than that of the axial force and will increase with eccentric force which cause the thickness of the vault increases the fastest and the value is the largest. The structure was subjected to compression at the beginning and gradually was changed to flexural tension with the increase in backfill height, so the section is mainly flexure tensile failure.

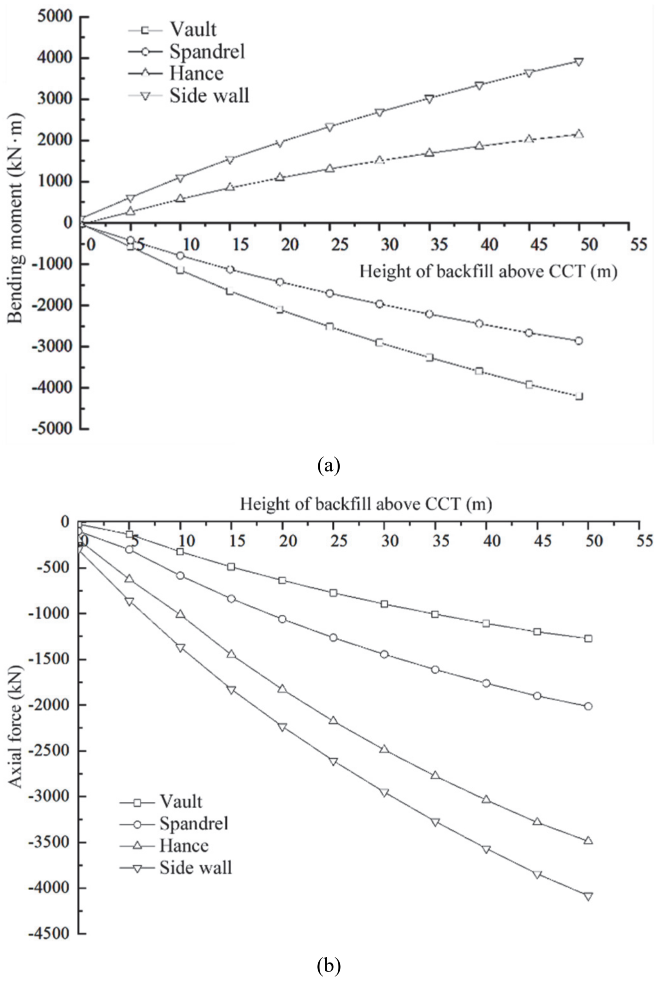

Fig. 3 Relationship between backfill height and (a) bending moment and (b) axial force

2.2.2 Thickness of Lining Structure

Figure 4 shows the relationship between the required thickness of a CCT's lining structure and the backfill height. The required thickness increases parabolically as the backfill height is increased. The required thickness from high to low is vault, spandrel, side wall, and hance; that is, the maximum thickness is at the vault. When the backfill height reaches 50 m, the required thicknesses of a CCT's lining structure are 4.35 m, 2.22 m, 1.91 m, and 1.21 m at the vault, spandrel, side wall, and hance, respectively. These required thicknesses are excessive, especially the thickness at the vault. This excessive thickness will result in cracks due to shrinkage after hardening and reduce the strength of the design. Therefore, either load reduction measures must be taken or the structural design must be modified to reduce the internal forces and required thickness of the lining structure. This study focused primarily on the structure and utilized soil-structure interactions to optimize this structural design. In addition, the influence of the backfill height on the thickness of the vault is greater than that of the thickness of intersection of lateral walls and the invert. The adjustment of the cross-sectional thickness at the vault can satisfy the stress requirements for the entire cross section of a CCT. Therefore, the thickness of the entire cross section can set uniform based on the thickness of the vault.

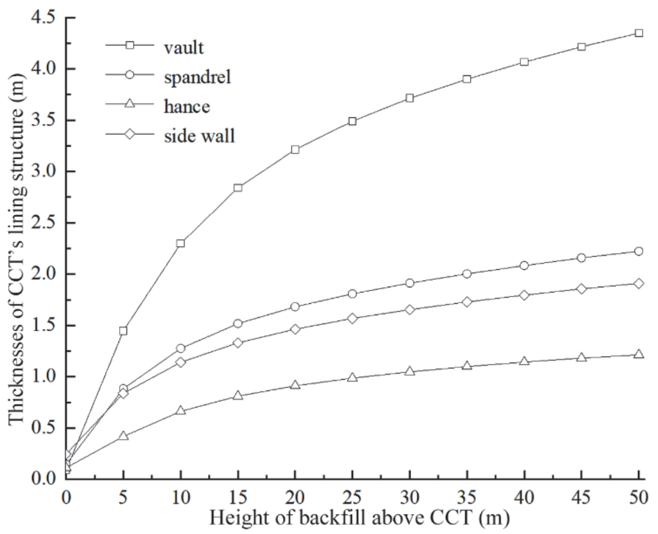

Fig. 4 Relationship between backfill height and required thicknesses of a CCT's lining structure at four different locations

2.3 Analysis of Cross-Sectional Design of Modified Lining Structure

The thickness and load-bearing capacity of a CCT are subjected to high backfill pressure, thus requiring improvement to the structural design to reduce the load. The improvement analysis here focused on modifying the conventional cross-section of a CCT. Figure 5 illustrates the cross-section modification that employs a vault optimization factor, $F = h/D$ (where h is arch height of CCT, and D is width of the CCT). Five different modified geometries, F = 0.54 (conventional), 0.7, 0.8, 1, and 1.2, were studied using numerical analysis. We obtained the thicknesses used in the finite element analysis through several iterative calculations to match the values assumed at the beginning of the analysis. In addition, in the structural optimization in this paper, the backfill height is a variable which can be changed. When F = 1.0, the thickness of the overburden soil will be increased to ensure that the backfill height remains the same.

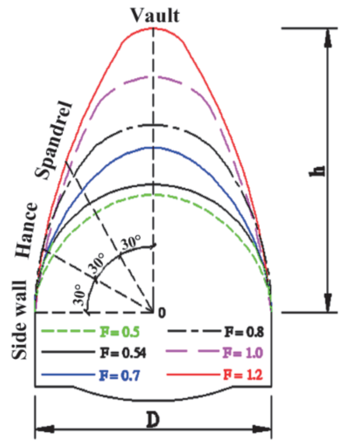

Fig. 5 Schematic of cross-section modifications to a CCT's lining structure

2.3.1 Internal Forces in Modified Cross-Sectional Design

Figure 6 shows the relationship between the vault optimization factor, F and the bending moment and axial force of the CCT lining structure at the vault, spandrel, hance and side wall. The transition points of the bending moment appear at approximately F = 1.0, and the transition point of the axial force appear at approximately F = 0.8 or F = 1.0 (Li *et al.* 2020b).

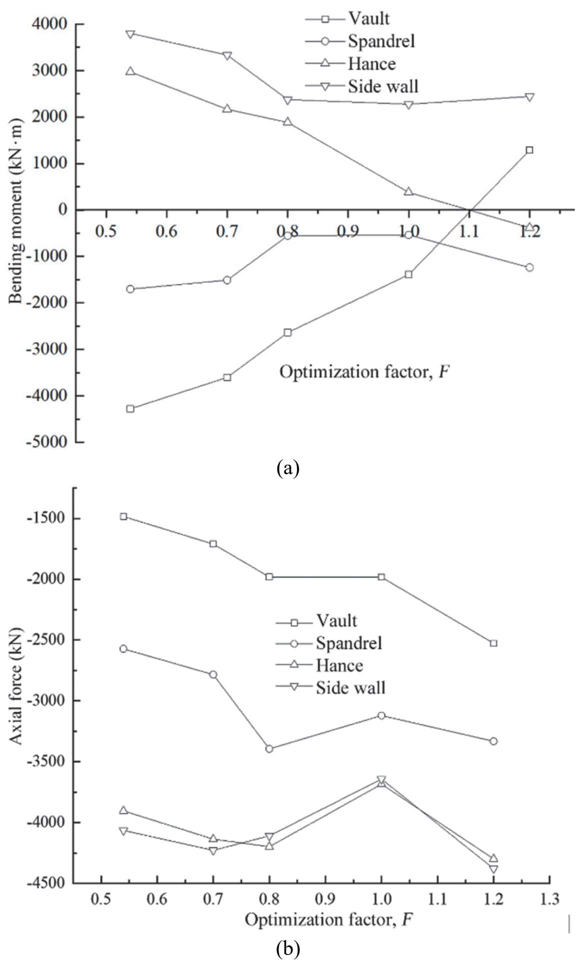

Fig. 6 Relationship between vault optimization factor, *F*, and (a) bending moment and (b) axial force (Li *et al.* 2020b)

2.3.2 Thickness of the Modified Lining Structure

Figure 7 presents a histogram to compare the required thicknesses of the CCT lining structure at the vault, spandrel, hance, and side wall when the height of the backfill is 50 m. The average thickness of the CCT's lining structure at each of the four locations has been found to be at its minimum if $F = 1.0$. (Li *et al.* 2020b) Therefore, an optimized modification of the cross-section of a CCT's lining structure is possible if $F = 1.0$.

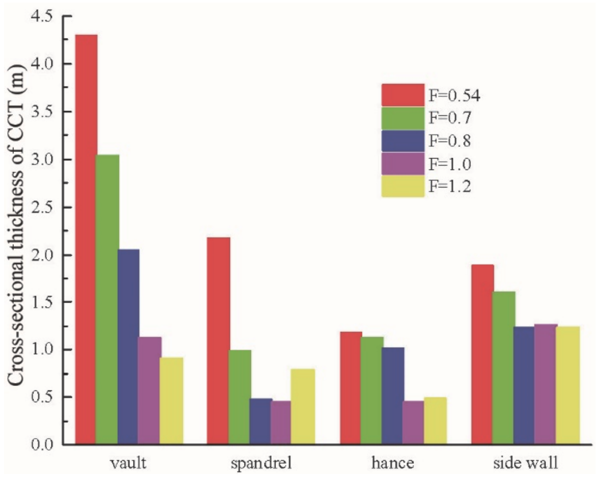

Fig. 7 Relationships among the required thicknesses of a CCT's lining structure at four locations and optimization factor, *F* (Li *et al.* 2020b)

2.3.3 Deformation of Modified Lining Structure

Figure 8 shows the relationship between the deformation of the CCT at two different locations, *i.e.*, the vault and the side wall, and the vault optimization factor, F, with a backfill height of 50 m. The deformation decreases from the scenario of $F = 0.54$ to that of $F = 1.0$ and then increases for $F = 1.2$. The deformations of the lining structure at these two locations are minimal when $F = 1.0$. Therefore, the optimization factor for the vault is $F = 1.0$ based on deformation subjected to earth pressure.

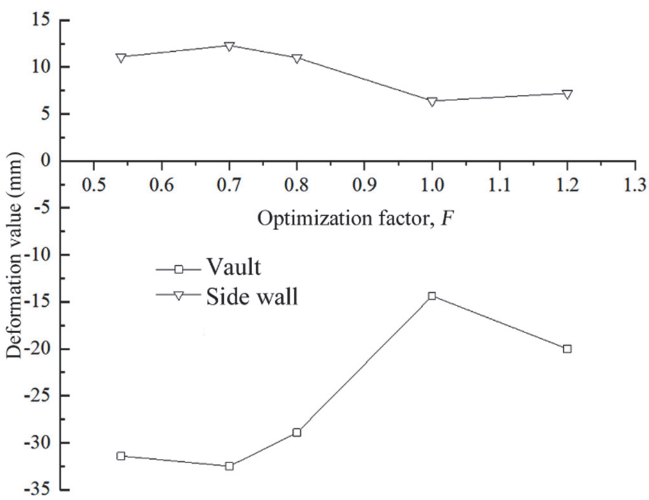

Fig. 8 Relationship between deformation and optimization factor, *F*, at two different locations

3. EXPERIMENTAL SETUP

The above results show that an optimized cross-sectional design works to reduce the required thickness of a CCT's lining structure and improve the safety of the structure. To validate the analysis results, we conducted physical model tests using both conventional and modified cross-section designs of CCTs.

3.1 Scale Analysis

Scale analysis is required to determine the suitable dimensions of a physical model for it to be applicable to a prototype. In this study, a physical model was used to simulate the numerical model. The geometrical similarity ratio, C_L, for the experimental model was determined to be 25.0, the density similarity ratio, C_r, was selected to be 1.0, and the other similarity ratios for the bending moment, C_M, and axial force, C_N, were selected to be 390625.0 and 15625.0, respectively (Li *et al.* 2020b).

3.2 Mechanical and Physical Properties of Materials

For the physical model tests, the mechanical and index properties for both the backfill soil and the lining structure needed to be determined. We obtained the backfill soil samples from a construction site and determined the physical and engineering properties via laboratory testing. We obtained the physical properties, including maximum dry density and optimal moisture content, from standard proctor testing following ASTM D698. We also conducted triaxial compression tests to determine the cohesion, c, internal friction angle, ϕ, and Young's modulus. Table 2 provides a summary of the laboratory test results for the backfill soil. The compressive strength of the concrete in CCT is 2.25×10^7 Pa. The gypsum was used to simulate the lining structure with C30 reinforced concrete, which satisfies the requirement for similarity between the prototype and the physical model (Li *et al.* 2020b).

Table 2 Physical properties of backfill soil

Optimum moisture content ω_{opt} (%)	Maximum dry density ρ_d (g/cm^3)	Unit weight γ (kN/m^3)	Cohesion c (kPa)	Internal friction angle ϕ (°)	Young's modulus E (MPa)
15.25	1.58	17.7	31.1	28.3	5.4

3.3 Experimental Model Scheme

Figure 9 shows the physical model test set-up with dimensions of 3,000 mm in length × 1,200 mm in width × 2,000 mm in height; Fig. 9(a) shows the physical model and Fig. 9(b) presents its cross-section. We tested two cases with different cross-sectional designs, conventional ($F = 0.54$) and modified ($F = 0.7$). For the conventional design, the dimensions of the CCT were 1,200 mm in length, 440 mm in height, 510 mm in width, and 30 mm in thickness with the maximum backfill heights of 0.5 m, which is equivalent to 12.5 m in the prototype (Li *et al.* 2014). For the modified design, the height was increased to 520 mm, while all the other dimensions remained the same as for the conventional design to ensure the optimization factor, $F = 0.7$. Strain sensors (BE120-20AA-P50) were set in the experiment, and the measured data of all the strain sensors installed in four different locations are used to calculate the internal force of CCT lining structure. The bending moment (M) and axial force (N) acting on these four positions are calculated by the following equation (Li *et al.* 2020b):

$$N = \frac{1}{2} E(\varepsilon_{in} + \varepsilon_{out})\, bh \tag{1}$$

$$M = \frac{1}{2} E(\varepsilon_{in} - \varepsilon_{out})\, bh^2 \tag{2}$$

E = elastic modulus of CCT lining structure; ε = strain of lining structure; b = width of cross section of lining structure; h = thickness of cross section of lining structure.

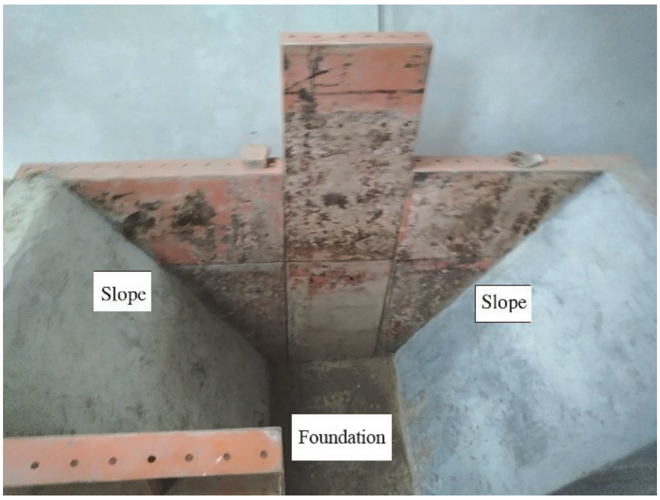

(a)

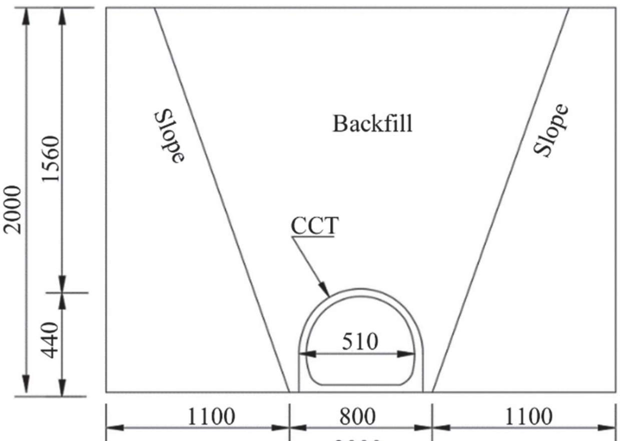

(b)

Fig. 9 Test set-up for (a) physical model and (b) cross-section of the physical model for *F* = 0.54

3.4 Experimental Results

In order to study the correctness of the theoretical calculation, the corresponding numerical model is established according to the similar proportion to calculate it. Figures 10(a) and 10(b) present comparisons of the physical model test results and the numerical simulations for the bending moments and axial forces, respectively, in a CCT's conventional cross-section lining structure (F = 0.54). Figures 11(a) and 11(b) similarly show comparisons for the modified CCT's lining structure (F = 0.70). The numerical analysis results for both tests align with the physical model test data for all the backfill heights studied, the average error between the experimental results and numerical analyses is approximately 5.0%. Meanwhile, compared to conventional cross-section of CCT's lining structure, the bending moment in modified CCT's lining structure is smaller, while the axial force is greater. Thus, if the modified cross-section of CCT's lining structure is used, the required thickness can be reduced under the same maximum height of backfill, or the allowable maximum backfill height can be increased.

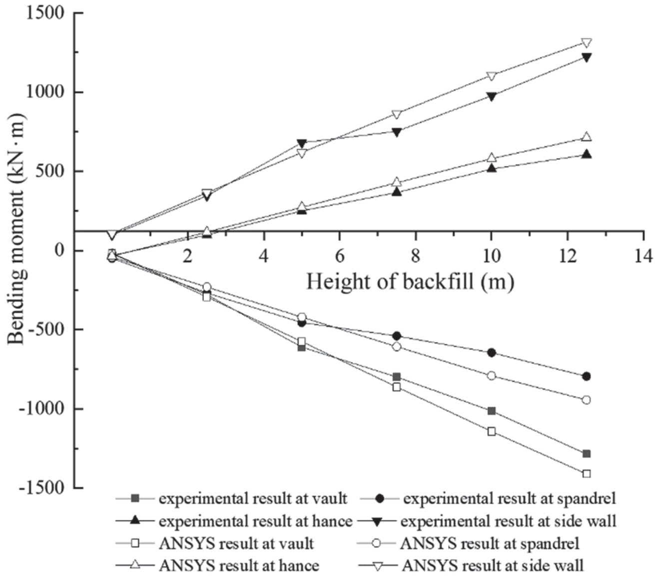

(a)

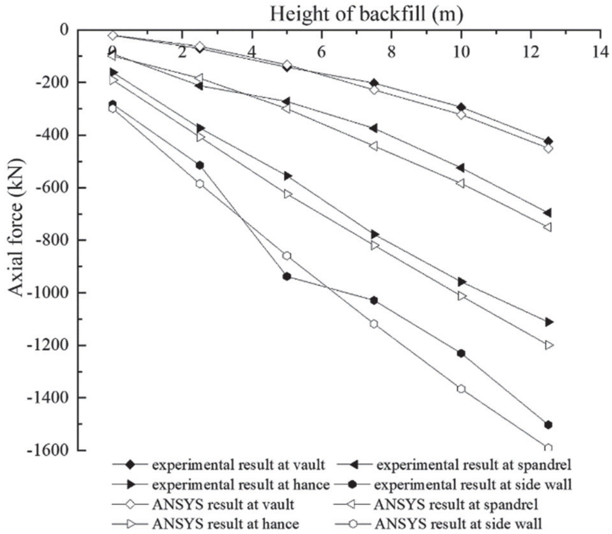

(b)

Fig. 10 Comparisons of numerical analysis and experimental results for (a) bending moments and (b) axial forces in a CCT's lining structure with conventional cross-section, *F* = 0.54

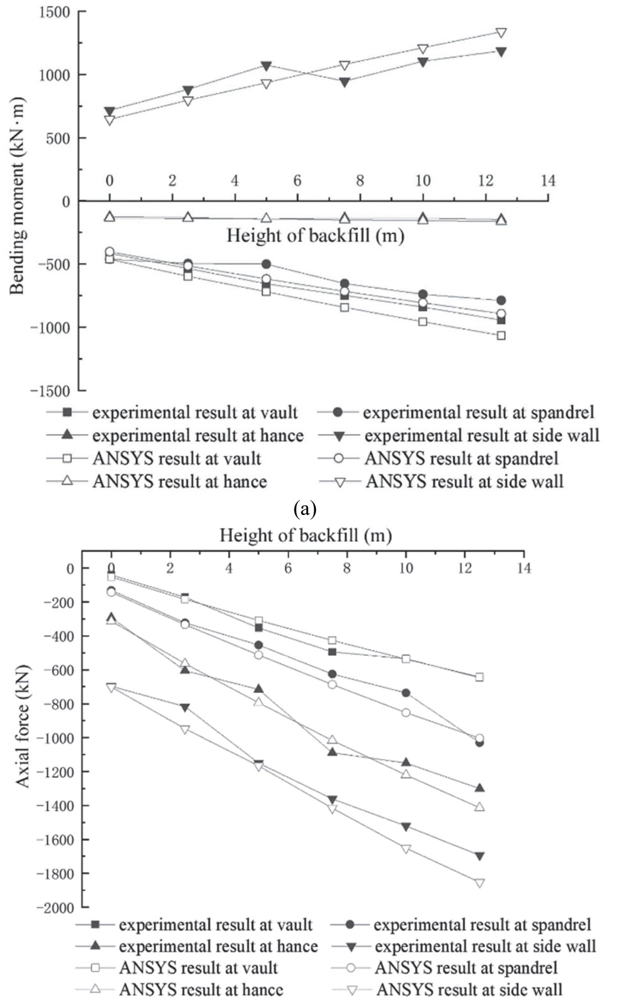

Fig. 11 Comparisons of numerical analysis and experimental results for (a) bending moments and (b) axial forces in a CCT's lining structure with modified cross-section, F = 0.7

4. DISCUSSION

The increasing rate of the bending moment is usually greater than that of the axial force when subjected to the earth pressure of backfill, which is unfavorable in the structural design of concrete. Concrete material has high compressive resistance and low tensile strength; therefore, its design thickness must be increased for CCTs. However, by modifying the cross-sectional design of a CCT's lining structure, the resultant bending moment can be significantly reduced and the axial force increased, thereby minimizing and optimizing the required thickness of the CCT.

This study focused on modifying the cross-sectional design of a CCT's lining structure without considering any load reduction measures for HFCCTs. The magnitude of the internal forces will vary if the cross-sectional design changes, which in turn will affect the required thickness of the CCT's lining structure. The thickness of the CCT in turn relates to the deformation of the CCT and the earth pressure around the CCT. Considering these multiple effects between the soil and the CCT, the internal forces and the thicknesses of the lining structure were obtained through iterative computations during the numerical analysis process. However, in the physical model tests, we used the same cross-section thickness due to geometric limitations. The analyses of lining structure internal forces are based on the same height of the backfill in both cases, i.e., conventional and modified.

The optimal CCT lining structure (F = 1.0) was not adopted in the physical model tests to ensure better data collection and concrete crack observations. Instead, we tested a modified cross-section using F = 0.7. The experimental results align with the numerical analysis results, and the physical model test results suggest that the modified cross-sectional design is favorable for reducing the designed thickness of the CCT's lining structure or increasing the allowable backfill height on top of the CCT.

Although physical model test and numerical analyses show that the thickness of the CCT can be reduced by optimizing the cross-sectional design, we did not consider several factors related to long-term stability, such as the creep of the backfill soil, degree of saturation, and the groundwater table. The research in this paper, the backfill is limited to loess in the Plateau Region of Northwest China, the slope is natural ditch. Moreover, this study did not address any possible post-construction problems that could be caused by the cross-section modifications, including the construction of CCTs and installation of equipment at the vault as well as the impact of seismic loads.

5. CONCLUSIONS

This study investigated the internal forces of HFCCTs with modifications to the structure to obtain an optimal cross-sectional design for CCTs. We evaluated the proposed geometric modifications using finite element analysis and conducted physical model tests to verify the numerical analysis results. The following conclusions can be drawn from this study.

1. The CCT's lining structure can be modified and optimized to enhance safety and reduce the required thickness of the CCT that is subject to backfilled earth pressure.
2. Modifications to a CCT's cross-sectional design can be made by increasing the proposed vault optimization factor, $F = h/d$. When h is increased, the arch of the CCT's lining structure becomes steeper and is favorable to reducing the bending moment and increasing the axial force. Due to the decrease in eccentric forces, the modified lining structure is subject to compression rather than flexural tension with an increase in backfill height.
3. Based on internal forces, required thickness, and deformations of the CCT's lining structure, the vault optimization factor is determined to be F = 1.0 for optimized cross-sectional modification.
4. For HFCCTs, the allowable backfill height can be significantly increased by modifying the cross-sectional design of the structure without requiring any load reduction measures for backfill soil.

FUNDING

This study was supported by the National Science Foundation of China (51868041, 51668036), Basic Research Innovation Group Project of Gansu Province (21JR7RA347), the Outstanding Graduate Student "Innovation Star" Project of Gansu Province

(2022CXZX-529), the Science and Technology Project of Gansu Province (21YF5GA050), the Industrial Support Plan of Education Department of Gansu Province (2021CYZC-28), and the Energy Geomechanics Laboratory at the University of North Dakota, U.S.A.

DATA AVAILABILITY

The data generated in this study are available from the corresponding author on reasonable request.

CONFLICT OF INTEREST STATEMENT

The authors declare that there is no conflict of interest.

REFERENCES

Ahmed, M., Tran, V., and Meguid, M.A. (2015). "On the role of geogrid reinforcement in reducing earth pressures on buried pipes." *Soils and Foundations*, **5**(33), 588-599. http://doi.org/10.1016/j.sandf.2015.04.010

El Naggar, H., Turan, A., and Valsangkar, A. (2015). "Earth pressure reduction system using geogrid-reinforced platform bridging for buried utilities." *Journal of Geotechnical and Geoenvironmental Engineering*, ASCE, **141**(6), 04015024. https://doi.org/10.1061/(asce)gt.1943-5606.0001307

Gu, A.Q., Guo, T.T., and Wang, X.P. (2005). "Experimental study on reducing load measurement using EPS of culvert under high-stacked soil." *Chinese Journal of Geotechnical Engineering*, **27**(5), 500-504 (in Chinese). http://doi.org/10.1007/s11769-005-0030-x

Larsen, N.G. and Hendrickson, J.G. (1962). "A practical method for constructing rigid conduits under high fills." *Proceedings of the 41st Annual Meeting of the Highway Research Board, Highway Research Board*, Washington, D.C, **41**, 273-280.

Li, S., Han, G.Q., Ho, I.H., Ma, L., Wang, Q.C., and Yu, B.T. (2020b). "Coupled effect of cross-sectional shape and load reduction on high-filled cut-and-cover tunnels considering soil-structure interaction." *International Journal of Geomechanics*, ASCE, **20**(7). http://doi.org/10.1007/s12205-020-1693-7

Li, S., Ho, I. H., Ma, L., Yao, Y.X., and Wang, C.D. (2019a). "Load reduction on high-filled cut-and-cover tunnel using discrete element method." *Computer and Geotechnics*, **114**, 103149. http://doi.org/10.1016/j.compgeo.2019.103149

Li, S., Li, S.Z., Wang, Q.C., Ma, L., Wang, Q.S., and Xu, W.Q. (2016b). "Unloading model test and numerical simulation analysis on high fill loess open cut tunnel with EPS." *Chinese Journal of Rock Mechanics and Engineering*, **35**(S1), 3394-3401 (in Chinese). http://doi.org/10.13722/j.cnki.jrme.2015.1401

Li, S., Ma, L., Ho, I.H., Wang, Q.C., Yu, B.T., and Zhou, P. (2019b). "Modification of vertical earth pressure formulas for high fill cut-and-cover tunnels using experimental and numerical methods." *Mathematical Problems in Engineering*, 2019, 19 p. https://doi.org/10.1155/2019/8257157

Li, S., Ma, L., Wang, Q.C., Li, S.Z., Li, J.X., and Zhang, Y.J. (2016a). "Model tests and numerical simulations of earth pressure for unloading structures of high fill open cut tunnel." *Chinese Journal of Geotechnical Engineering*, **38**(4), 636-642 (in Chinese). http://doi.org/10.11779/CJGE201604007

Li, S., Wang, Q.C., Ma, L., Li, J.X., and Li, W.L. (2014). "Model analysis of earth pressure load reduction and soil arch effect for high fill open cut tunnel in loess area." *China Civil Engineering Journal*, **47**(7), 118-125 (in Chinese). http://doi.org/10.15951/j.tmgcxb.2014.07.040

Li, S., Yao, Y.X., Ho, I.H., Ma, L., and Wang, Q.C. (2020a). "Coupled effect of expanded polystyrene and geogrid on load reduction for high-filled cut-and-cover tunnels using the discrete element method." *International Journal of Geomechanics*, ASCE, **20**(6). https://doi.org/10.1061/(asce)gm.1943-5622.0001683

Liedberg, N.S.D. (1997). "Load reduction on a rigid pipe: Pilot study of a soft cushion installation." *Transportation Research Record*, **1594**, 217-223. http://doi.org/110.3141/1594-25

Marston, A. (1922). *Second Progress Report to the Joint Concrete Culvert Pipe Committee*. Iowa Engineering Experimental Station, Ames, Iowa.

McAffee, R.P. and Valsangkar, A.J. (2004), "Geotechnical properties of compressible materials used for induced trench construction." *Journal of Testing and Evaluation*, **32**(2), 143-152. http://doi.org/10.1520/JTE11924

McAffee, R.P. and Valsangkar, A.J. (2008). "Field performance, centrifuge testing, and numerical modelling of an induced trench installation." *Canadian Geotechnical Journal*, **45**(1), 85-101. https://doi.org/10.1139/t07-086

McGuigan, B.L. and Valsangkar, A.J. (2011a). "Earth pressures on twin positive projecting and induced trench box culverts under high embankments." *Canadian Geotechnical Journal*, **48**(2), 173-185. https://doi.org/10.1139/t10-058

McGuigan, B.L. and Valsangkar, A.J. (2011b). "Field monitoring and analysis of twin 3660 mm inside diameter induced trench culverts installed under 21.7 m of fill." *Canadian Geotechnical Journal*, **48**(5), 781-794. https://doi.org/10.1139/t11-002

McGuigan, B.L. and Valsangkar, A.J. (2010). "Centrifuge testing and numerical analysis of box culverts installed in induced trenches." *Canadian Geotechnical Journal*, **47**(2), 147-163. https://doi.org/10.1139/t09-085

Meguid, M.A., Hussein, M.G., Ahmed, M.R., Omeman, Z., and Whalen, J. (2017). "Investigation of Soil-geosynthetic-structure Interaction Associated with Induced Trench Installation." *Geotextiles and Geomembranes*, **45**(4), 320-330. https://doi.org/10.1016/j.geotexmem.2017.04.004

Mehrjardi, G.T., Moghaddas Tafreshi, S.N., and Dawson, A.R. (2013). "Pipe response in a geocell-reinforced trench and compaction considerations." *Geosynthetics International*, **20**(2), 105-118. https://doi.org/10.1680/gein.13.00005

Palmeira, E.M. and Andrade, H.K.P.A. (2010). "Protection of buried pipes against accidental damage using geosynthetics." *Geosynthetics International*, **17**(4), 228-241. https://doi.org/10.1680/gein.2010.17.4.228

Roh, H.S., Choi, Y.C., and Kim, S.H. (2000). "Earth pressures on culvert during compaction of backfill." *Proceedings of the International Society for Rock Mechanics Symposium*, Melbourne, Australia.

Sladen, J.A. and Oswell, J.M. (1988). "The induced trench method—A critical review and case history." *Canadian Geotechnical Journal*, **25**(3), 541-549. https://doi.org/10.1139/t88-059

Spangler, M.G. (1958). "A practical application of the imperfect ditch method of construction." *Proceedings of the Thirty-*

Seventh Annual Meeting of the Highway Research Board, Highway Research Board, Washington, D.C., **37**, 271-277.

Sun, L., Hopkins, T.C., and Beckham, T.L. (2009). *Reduction of Stresses on Buried Rigid Highway Structures Using the Imperfect Ditch Method and Expanded Polystyrene (Geofoam)*. Kentucky Transportation Center, Report No. KTC-07-14-SPR228-01-1F, University of Kentucky, Kentucky, USA, 49.

Taylor, R.K. (1973). *Induced Trench Method of Culvert Installation*. Highway Research Record No. 52, Highway Research Board, Washington, D.C., 15-31.

Van Eekelen, S.J.M., Bezuijen, A., and van Tol, A.F. (2013). "An analytical model for arching in piled embankments." *Geotextiles and Geomembranes*, **39**(1), 78-102. http://doi.org/10.1016/j.geotexmem.2013.07.005

Vaslestad, J. (1990). *Soil Structure Interaction of Buried Culverts*. Ph.D. Dissertation, Norwegian Institute of Technology, Norway.

Vaslestad, J., Johansen, T.H., and Holm, W. (1993). "Load reduction on rigid culverts beneath high fills: Long-term behavior." *Transportation Research Record*, 1415, Transportation Research Board, Washington, D.C., 58-68.

Villard, P., Huckert, A., and Briançon, L. (2016). "Load transfer mechanisms in geotextile reinforced embankments overlying voids: Numerical approach and design." *Geotextiles and Geomembranes*, **44**(3), 381-395. https://doi.org/10.1016/j.geotexmem.2016.01.007

Vladimir, H., Jan, E., and Lumir, M. (2013). "Shape optimization of concrete buried arches." *Engineering Structures*, **48**. http://doi.org/10.1016/j.engstruct.2012.11.037

Zaeske, D. (2001). *Zur wirkungsweise von unbewehrten und bewehrten mineralischen Tragschichten über pfahlartigen Gründungselementen. Schriftenreihe Geotechnik*. Kassel, Germany: Univ. of Kassel (in German).

Zhang, W., Liu, B., and Xie, Y. (2006). "Field test and numerical simulation study on the load reducing effect of EPS on the highly filled culvert." *Journal Highway Transportation Research Reseach Development China*, **23**(12), 54-57. http://doi.org/10.3969/j.issn.1002-0268.2006.12.013

Zheng, J.J., Ma, Q., and Zhang, J. (2011). "Calculation of vertical earth pressure on load reduction Culverts under embankments by reinforcement." *Chinese Journal of Geotechnical Engineering*, **33**(7), 1135-1141 (in Chinese). http://doi.org/10.1631/jzus.B1000185